ACS OMEGA

Open Access

http://pubs.acs.org/journal/acsodf

Article

Comprehensive Characterization of Commercial Reverse Osmosis Membranes through High-Temperature Cross-Flow Filtration

Pooria Karami, Sadegh Aghapour Aktij, Kazem Moradi, Masoud Rastgar, Behnam Khorshidi, Farshad Mohammadtabar, John Peichel, Michael McGregor, Ahmad Rahimpour, Joao B. P. Soares, and Mohtada Sadrzadeh*

Cite This: *ACS Omega* 2024, 9, 1990−1999

Read Online

ACCESS | Metrics & More | Article Recommendations

ABSTRACT: Developing thermally stable reverse osmosis membranes is a potential game-changer in high-temperature water treatment. In this work, the performance of three commercial reverse osmosis membranes was evaluated with a series of high-temperature filtrations. The membranes were tested with different filtration methodologies: long-term operation, cyclic tests, controlled stepwise temperature increment, and permeability tests. The morphological and physiochemical characterizations were performed to study the impact of high-temperature filtration on the membranes' chemical composition and morphological characteristics. An increase in the temperature deteriorated the membrane performance in terms of water flux and salt rejection. Flux decline at high temperatures was recognized as the primary concern for high-temperature filtrations, restricting the applications of commercial membranes for long-term operations. This research provides valuable insights for researchers aiming to thoroughly characterize reverse osmosis membranes at high temperatures.

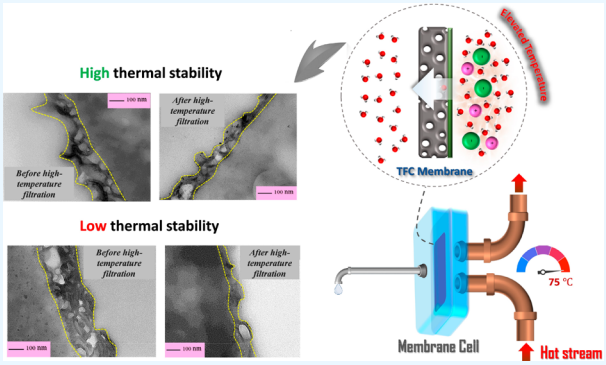

1. INTRODUCTION

Many industries produce a massive amount of contaminated water at high temperatures, which must be treated, recycled, and reused. Seasonal and daily temperature variations may also affect the influent water temperature at the treatment facilities.[1,2] For example, in the province of Alberta, Canada, the in situ oil extraction process produces highly contaminated water at high temperatures. Steam-assisted gravity drainage (SAGD), as the front-runner technology for oil extraction in Alberta, consumes 2−3 barrels of water to extract one barrel of oil. Most water treatment technologies provide optimal performance at room temperature.[3,4] In the case of membrane filtration, the low thermal stability of most commercial polymeric membranes is the main limiting factor. Therefore, the hot wastewater must be cooled down before being accommodated into a membrane filtration process, which enhances the capital and operating costs when dealing with hot streams.[5,6] Given the above, there is a growing demand for developing water treatment techniques that operate at high temperatures and thus improve the heat integration of the overall process. From the cost and energy savings viewpoint, the membrane must perform at the highest allowable temperature.

Polyamide thin-film composite (TFC), the industry-standard multilayer structure of reverse osmosis and nanofiltration membranes, is widely used in different separation applications like municipal and industrial wastewater reclamation or seawater desalination.[7−10] TFC membranes are commonly developed by coating an ultrathin cross-linked polyamide layer on the top of microporous support.[11,12] The nanoscale polyamide layer is formed via an interfacial polymerization reaction between a diamine-containing monomer (like m-phenylenediamine) and a triacyl chloride monomer (like trimesoyle chloride). Three functional groups on the trimesoyle chloride monomer form a 3-dimensional cross-linked polyamide network necessary for high salt rejection from water. Any change in monomer type, interfacial reaction time, or peripheral condition can largely impact the final film characteristics.[13,14]

Most commercial polymeric TFC membranes are recommended to be used below 45 °C. The TFC membranes exhibit unfavorable separation performance, particularly when exposed to high temperatures above 45 °C. The primary challenge of

Received: November 22, 2023
Revised: December 1, 2023
Accepted: December 6, 2023
Published: December 21, 2023

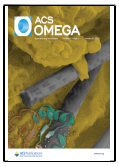

https://doi.org/10.1021/acsomega.3c09331
ACS Omega 2024, 9, 1990−1999

Figure 1. Commercial polyamide TFC membranes used in this study: Veolia AG and Veolia AK, which are standard and low-pressure brackish water reverse osmosis membranes, and Veolia AD, which is designed for delivering high NaCl rejection under seawater operating conditions.

high-temperature water filtration for reverse osmosis membranes is the flux decline at elevated temperatures. This decline in flux not only compromises separation efficiency but also presents economic challenges. In order to address the flux decline, it is essential to increase the operating pressure to sustain the initial flux. This, in turn, adds to the operational costs of the reverse osmosis process. Consequently, the direct application of TFC membranes faces limitations in effectively treating streams such as hot condensate, boiler-water blowdown, textile and sugar effluents, laundry wastewater, annealing baths, high-temperature mining wastewater, and produced water in the oil and gas industries.[2] In some food industries, water streams must be kept at an elevated temperature (up to 90 °C) to prevent biological contamination.[15] In the pharmaceutical processes, the membranes should be exposed to high-temperature (up to 95 °C) water streams for sanitization. This operation is mostly performed at hydraulic pressures as low as 60 psi for several hours. In some industries, the saturation of aqueous solution with different salts necessitates keeping the unit temperature at a high value; otherwise, the solubility limit of critical compounds may overpass. In the SAGD process, the produced water temperature is as high as ∼150 °C, and a large amount of energy is wasted for cooling down the produced water from this temperature to below 70 °C (or lower) for water treatment and then heating it again up to ∼220 °C to produce steam.[16]

It is reported that increasing the temperature is favorable for water recovery but has a deteriorating effect on the separation performance of the membranes. Increasing the filtration temperature affects the membrane properties, solvent, and solute mobilities.[17] Some research works investigated the effect of temperature on solute transport through nanofiltration membranes.[18] Nanofiltration polyamide membranes showed less rejection of uncharged solutes at higher temperatures. This reduction is justified by increasing the pore radius of membranes at elevated temperatures, leading to less steric exclusion of solutes. Roy et al.[17] studied the effect of temperature on the transport of monovalent and divalent ions through nanofiltration membranes. Solute transport through the membranes, with three mechanisms, including convection (ion movement by solvent flow), diffusion (ion movement by concentration gradient), and electromigration (ion movement by a potential gradient), was found to be enhanced at higher temperatures. Higher temperatures also reduce the dielectric exclusion of solutes because the pore dielectric constant at elevated temperatures decreases. The authors concluded that higher solute transport at elevated temperatures could be due to a change in membrane properties (e.g., increased polymer chain mobility at higher temperatures), lower solvent viscosity (enhanced convection flow), and higher ion diffusivity. However, our recent studies on fabricating novel thermally stable reverse osmosis membranes[7,19,20] revealed an increase in NaCl rejection at higher temperatures. Such an opposite trend of NaCl rejection in reverse osmosis membranes compared to nanofiltration membranes can be justified by the difference in the solute transport mechanism through the dense polyamide layer of these two types of membranes. We attributed the increase in NaCl rejection with temperature to primarily the plasticizing effect of the temperature on collapsing internal free volumes of the polyamide structure. Indeed, physical or chemical changes of polymeric materials with temperature should be considered in justifying reverse osmosis membranes' performance at elevated temperatures. The thermal stability of a polymeric membrane is found to be highly dependent on the polymer material properties, such as aromaticity, cross-linking degree, chain interactions, and stiffing functional groups.[2,21] Improving the cross-link density of the polyamide layer by using new monomers and fabricating a fully aromatic polyamide structure has already been investigated.[19,22] Further studies showed that incorporating some inorganic fillers like TiO_2, carbon nanotube (CNT), and nanodiamonds could improve the thermal and mechanical characteristics of the TFC membranes.[20,23−25] Nevertheless, the first step in designing state-of-the-art thermally stable reverse osmosis membranes is to develop laboratory protocols for high-temperature testing similar to those for industrial reverse osmosis operations.

This study aims to test three flat-sheet commercial reverse osmosis membranes in a simulated operational environment of SAGD operation at high temperatures (70−80 °C). The main objectives are to (i) establish an understanding regarding the thermal stability of available commercial reverse osmosis membranes in the market, (ii) suggest protocols for high-temperature testing of reverse osmosis membranes, and (iii) provide insights regarding the fabrication of thermally stable reverse osmosis TFC membranes.

https://doi.org/10.1021/acsomega.3c09331
ACS Omega 2024, 9, 1990−1999

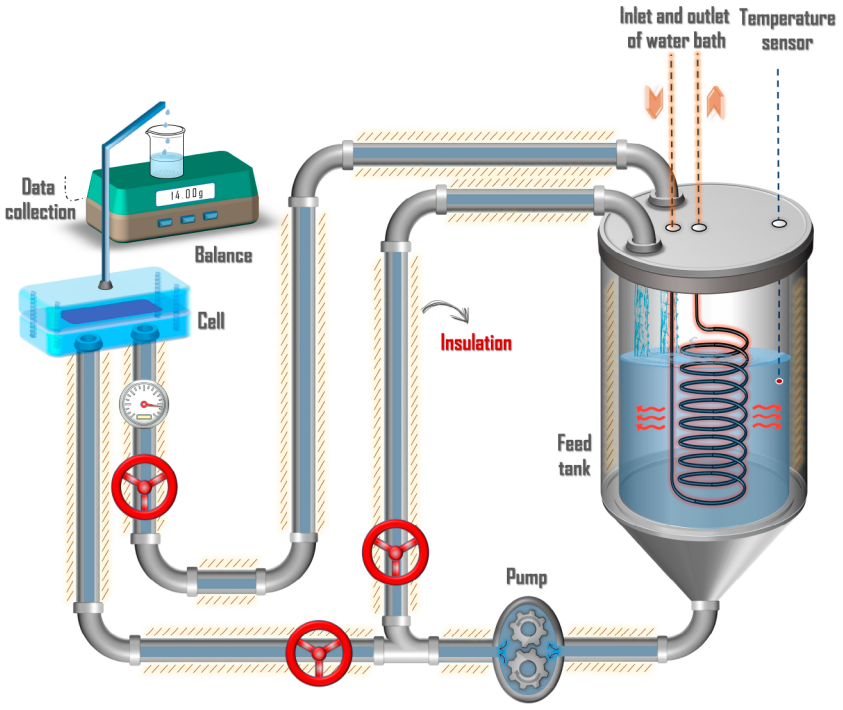

Figure 2. High-temperature reverse osmosis cross-flow filtration setup. The feed tank and all of the pipes were insulated to minimize heat loss during the high-temperature filtrations.

2. MATERIALS AND METHODS

2.1. Materials. Veolia AG, Veolia AK, and Veolia AD as flat-sheet commercial polyamide TFC membranes were all supplied from Veolia Water Technologies & Solutions (MN, USA) (see Figure 1). In this paper, we used AG, AK, and AD symbols to label these membranes. The flat-sheet membranes were used for filtration after overnight soaking the coupon samples in isopropanol (IPA) and water solution with a volume ratio of 1:4. Sodium chloride (NaCl) (>99%) was purchased from Fisher Scientific and used to prepare the feed solution. Deionized (DI) water, obtained from a Milli-Q ultrapure water purification system (Synergy 185, 18.2 MΩ cm, EMD Millipore Corp., Billerica, MA), was used for all experiments.

2.2. Experimental Methodologies. *2.2.1. Evaluation of the Separation Performance of Membranes at High Temperature.* High-temperature filtration tests were carried out by using a cross-flow filtration setup (Sterlitech Corp., USA). The setup is equipped with a circulating water bath (Isotemp3013, Fisher Scientific) to control the feed solution temperature. The mass of collected permeate was continuously recorded by using a digital weighing balance (ME4002, Mettler Toledo, USA). The permeate flux was calculated with the following equation:

$$J_W = \frac{\Delta m}{\rho A_m \Delta t} \quad (1)$$

where Δm is the mass difference of the collected permeate solution, ρ is water density, A_m is the effective membrane area (20.6×10^{-4} m^2), and Δt is the time interval. To evaluate the NaCl rejection, the conductivity of the feed and permeate solution was measured using a conductivity meter (Accumet AR50, Fisher Scientific). Then the conductivity data was converted to the NaCl concentration using a calibration curve. The salt rejection was calculated using the following formula:

$$R(\%) = \left(\frac{C_F - C_P}{C_F}\right) \times 100 \quad (2)$$

where C_F and C_P are the NaCl concentration of the feed and permeate solution, respectively. All of the filtration setup elements were insulated to reduce heat loss during the high-temperature experiments. Figure 2 illustrates a schematic of a laboratory cross-flow filtration setup.

High-temperature cross-flow filtration tests were conducted at different modes to comprehensively study the behavior of commercial reverse osmosis membranes when they are exposed to high temperatures: (i) long-term high-temperature filtrations, (ii) cyclic tests, (iii) stepwise temperature increments by adjusting pressure, and (iv) permeability measurements at different temperatures.

i. Long-Term High-Temperature Filtrations. The filtration started with pure water at room temperature for 30 min. Then, a 2000 ppm of NaCl solution was added to the feed tank. The feed temperature was steadily increased to 75 °C. The filtration at 75 °C continued for 7 days to evaluate the stability of the membranes. The water levels in the feed tank and water circulator were constantly monitored to eliminate possible high-temperature evaporation. The transmembrane pressure and concentrate flow rate were set to 90 psi and 3 L/min during filtration.

ii. Cyclic Tests. We conducted cyclic experiments to simulate real industrial high-temperature applications that involve on/off operations. The filtration started with pure water at 25 °C. Then a 2000 ppm of NaCl solution was added after 30 min. The operation temperature was increased continuously from 25 to 75 °C and kept constant for 4 h. Then, the operating temperature was decreased to 25 °C. The next day, the feed solution was heated again to 75 °C, and the filtration continued for 4 h at elevated temperatures. The same

https://doi.org/10.1021/acsomega.3c09331
ACS Omega 2024, 9, 1990−1999

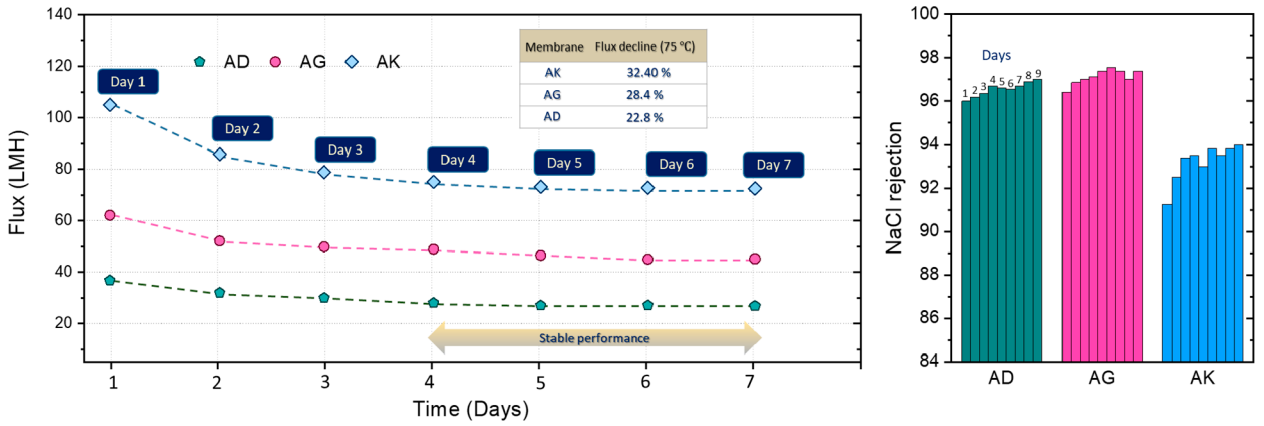

Figure 3. Water flux and NaCl rejection of the AK, AG, and AD membranes in a long-term (7 days) filtration. The permeate samples at high temperature were collected and allowed to be cooled to room temperature for conductivity measurement.

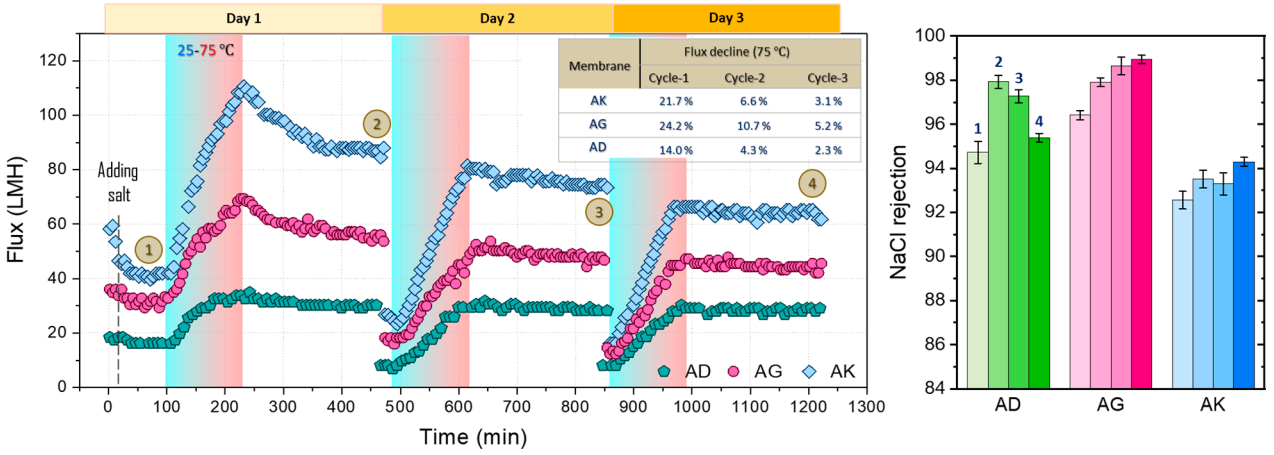

Figure 4. Water flux and salt rejections of cyclic operations of AK, AG, and AD membranes in 3 days. The flux decline of the membranes at 75 °C for each cycle was calculated and listed in a table in the first panel. After finishing each cycle, the feed solution was cooled slowly overnight.

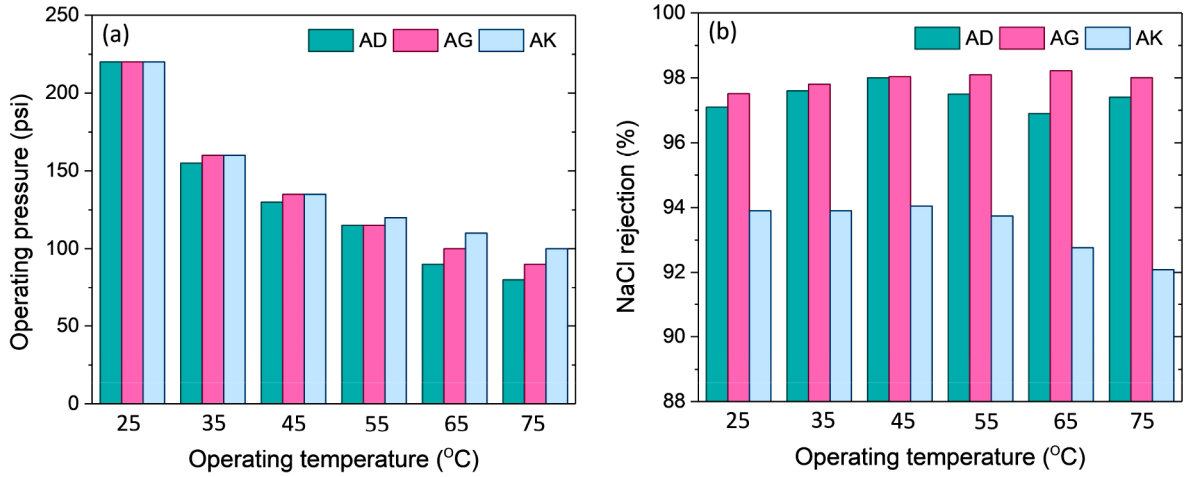

Figure 5. (a) The trans-membrane pressure of the membranes at different operating temperatures. The water flux was set to 35 LHM, 72 LMH, and 112 LMH for AD, AG, and AK membranes, respectively, and (b) NaCl rejection of the membranes at different temperatures.

cycle was repeated for the third day. The trans-membrane pressure was set to 90 psi in all cycles.

iii. Stepwise Temperature Increment by Adjusting the Pressure. To study the effect of the temperature on the performance of the membranes exclusively, we employed this technique to minimize the impact of operating pressure on membrane performance at elevated temperatures. The trans-membrane pressure was adjusted at each temperature level to deliver the same water flux. Filtration started with pure water at 25 °C for 30 min. Then, a 2000 ppm of NaCl solution was added to the feed tank. The feed temperature increased with 10 °C intervals to 75 °C. The pressure was adjusted

https://doi.org/10.1021/acsomega.3c09331
ACS Omega 2024, 9, 1990−1999

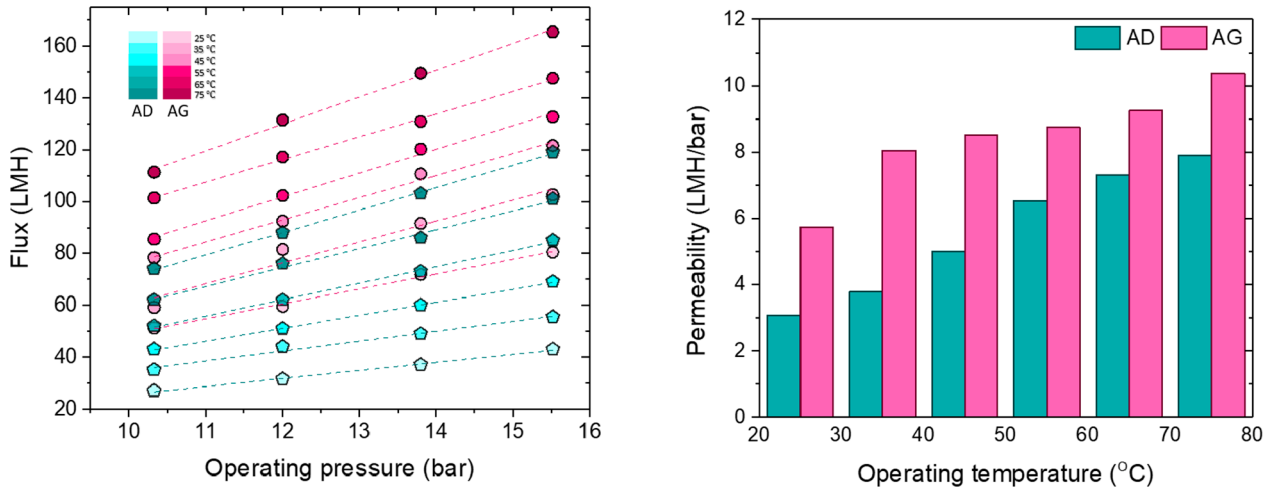

Figure 6. Water permeability of membranes at different temperatures. The permeability was reported by calculating the slope of the flux/pressure curves.

(decreased) at each temperature level to have the same permeate flux.

iv. Permeability Measurement at Different Operating Temperatures. The pure water filtration was conducted at different temperatures (25, 35, 45, 55, 65, and 75 °C), and the permeability of the membranes was calculated. The permeate flux at four operating pressures was measured at each temperature level. The slope of water flux vs operating pressure gives the permeability of the membranes. For each temperature, a new membrane coupon was used.

2.2.2. Morphological Analysis of the Membranes. The top surface morphological features of the TFC membranes were evaluated by field-emission scanning electron microscopy (FESEM, Zeiss Sigma 300 VP). The thickness of the polyamide selective layer was evaluated with cross-sectional transmission electron microscopy (TEM, Philips/FEI Morgagni 268) images. The effect of the temperature on the topography of the polyamide layer was further studied with atomic force microscopy (AFM, Bruker Dimension Icon, USA) in tapping mode at room temperature. The three-dimensional AFM images along with the roughness data, including average roughness (R_a) and root-mean-square roughness (R_q), were obtained by the nasoscope image analysis software.

2.2.3. Chemical Composition of the Membranes. Attenuated total reflectance-Fourier transform infrared spectroscopy (ATR-FTIR) was conducted to determine the chemical composition of the polyamide layer. The FTIR spectra were recorded with an Agilent Technologies Cary 600 series FTIR spectrometer over the range of 400−4000 cm^{-1} at 4 cm^{-1} resolution at the transmittance mode and after 30 scans.

3. RESULTS AND DISCUSSION

3.1. High-Temperature Filtrations of Flat-Sheet Membranes. *3.1.1. Long-Term Performance of the Membranes at High Temperature.* Figure 3 illustrates the water flux and NaCl rejection of the commercial reverse osmosis membranes at 75 °C. The performance of the membranes was evaluated for 7 days. The NaCl rejection was measured at high-temperature filtration each day. All reverse osmosis membranes experienced flux decline during 7 days of filtration. AD membrane showed a 22.8% flux decline (8 LMH) at high

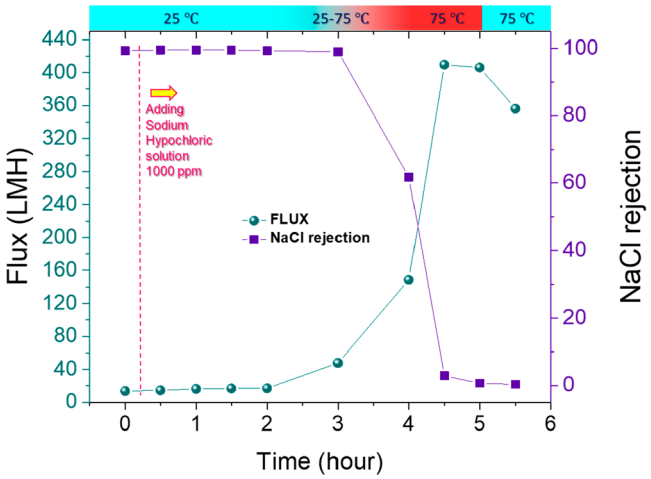

Figure 7. Water flux and NaCl rejection of the AD membrane when the feed solution contained 1000 ppm of sodium hypochlorite.

temperatures, indicating its high stability in a long-term operation. However, the brackish water membranes (AK and AG) showed a 32.40% and 28.4% flux decline, respectively. The NaCl rejection for all three membranes increased over the 7-day experiment. AK membrane had a greater improvement in NaCl rejection compared to AD and AG membranes. The enhancement in NaCl rejection over time can be attributed to the effect of temperature on the polymeric structure of the selective layer. As the membrane experienced a consistent hydraulic pressure at elevated temperatures, it underwent compaction, reducing free volume within the polyamide matrix. The compaction of the polymeric structure at elevated temperatures adversely impacts water flux at 75 °C but enhances the salt rejection of the membranes.

The flux decline at high temperatures can be explained by the low thermal resistance of the polymeric structures of the membranes. The plasticizing effect of the temperature on the membranes subjected to a permanent hydraulic pressure leads to the collapse of the membrane structure's internal voids, consequently lowering the free volume. The AD membrane, designed for seawater desalination (800 psi operating pressure), possesses a dense polyamide layer with a low permeability. The rigid selective layer resisted thermal stresses

https://doi.org/10.1021/acsomega.3c09331
ACS Omega 2024, 9, 1990−1999

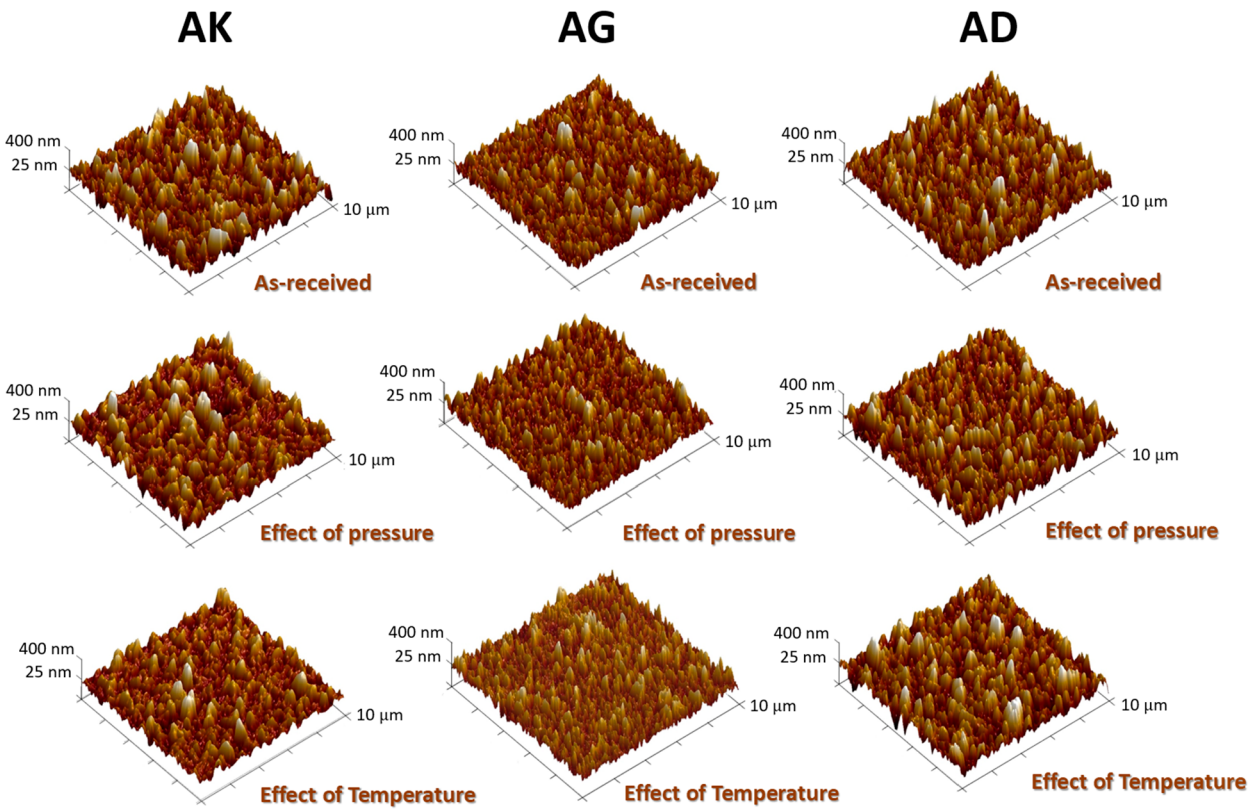

Figure 8. Top surface 3D topography AFM images of as-received membranes, membranes after filtration at room temperature, and membranes after filtration at a high temperature.

Table 1. Roughness Data, Including Ra: Average Roughness and Rq: Root Mean Square Roughness of AK, AG, and AD Membranes

	R_a (nm)			R_q (nm)		
Membrane	As-received	Pressure-effect	Temp-effect	As-received	Pressure-effect	Temp-effect
AK	76.2	70.3	61.5	96.6	92.2	79.2
AG	59.9	57.7	58.5	76.5	73.5	73.1
AD	72.3	70	83.6	91.2	88.5	105.7

better at elevated temperatures than brackish water membranes (AG and AK), with selective layers more prone to structural variations at high temperatures.

3.1.2. Cyclic Tests. Figure 4 demonstrates the water flux and NaCl rejection of reverse osmosis TFC membranes in cyclic operations in 3 days. In the first cycle, the flux of the membranes increased with an increase in the temperature. The water flux reached the highest value with different rates, where AG and AD showed the lowest and highest ratios of water flux at 75 °C to the water flux at 25 °C, respectively. We noticed that the membranes with a higher flux ratio in the transition zone (25−75 °C) had a lower flux decline at 75 °C. The NaCl rejection had an increasing trend for all of the membranes when the temperature increased. At higher temperatures, the diffusion rate of all feed solution components, including water molecules, through the membrane film increases. Besides, temperature enhancement reduces the solvent viscosity and density, facilitating fast permeation through the membrane. These two phenomena enhance the water flux during filtration in the temperature transition zone.[19,26,27] Furthermore, at high temperatures, the intensified segmental motions of the polymeric network allow the formation of more water channels inside the polyamide membranes.[20] Enhancement of the NaCl rejection at 75 °C might be attributed to the different impact of the temperature on the diffusion of water molecules and NaCl ions at high temperatures. As the water permeation rate is faster than the salt passage at high temperatures, the rejection percentage increases, i.e., permeate water quality is improved when filtering hot feed streams.[28]

On days 2 and 3, the flux decline at 75 °C decreased for all of the membranes. This observation implies that high temperature had a weaker effect on the heat-treated membranes. Another indication of the more stable performance of the membranes in cycles 2 and 3 is a more linear flux increment in the temperature transition zones (25−75 °C). A linear trend of water flux during the temperature increment can be explained by the smaller structural variation of polyamide due to thermal stresses. The water flux of the membranes at 25 °C had a decreasing trend for all of the membranes in three cycles as well. The NaCl rejection was measured at points 1−4, as shown in Figure 4 (panel 1). The rejection for all of the membranes increased at higher temperatures. However, NaCl rejection of the AD membrane decreased in cycles 2 and 3.

3.1.3. Stepwise Temperature Increment. Figure 5 shows the water flux and NaCl rejection of the membranes in the range of 25−75 °C with 10 °C intervals. The operating pressure was adjusted to deliver the same initial water flux at each temperature level. The initial flux for AD, AG, and AK was set to 35 LHM, 72 LMH, and 112 LMH, respectively. As observed in Figure 5, the operating pressure decreased with an increase in the temperature. The NaCl rejections for AD and AG showed low variations by elevating the temperatures. However, the salt rejection of AK decreased at higher

https://doi.org/10.1021/acsomega.3c09331
ACS Omega 2024, 9, 1990−1999

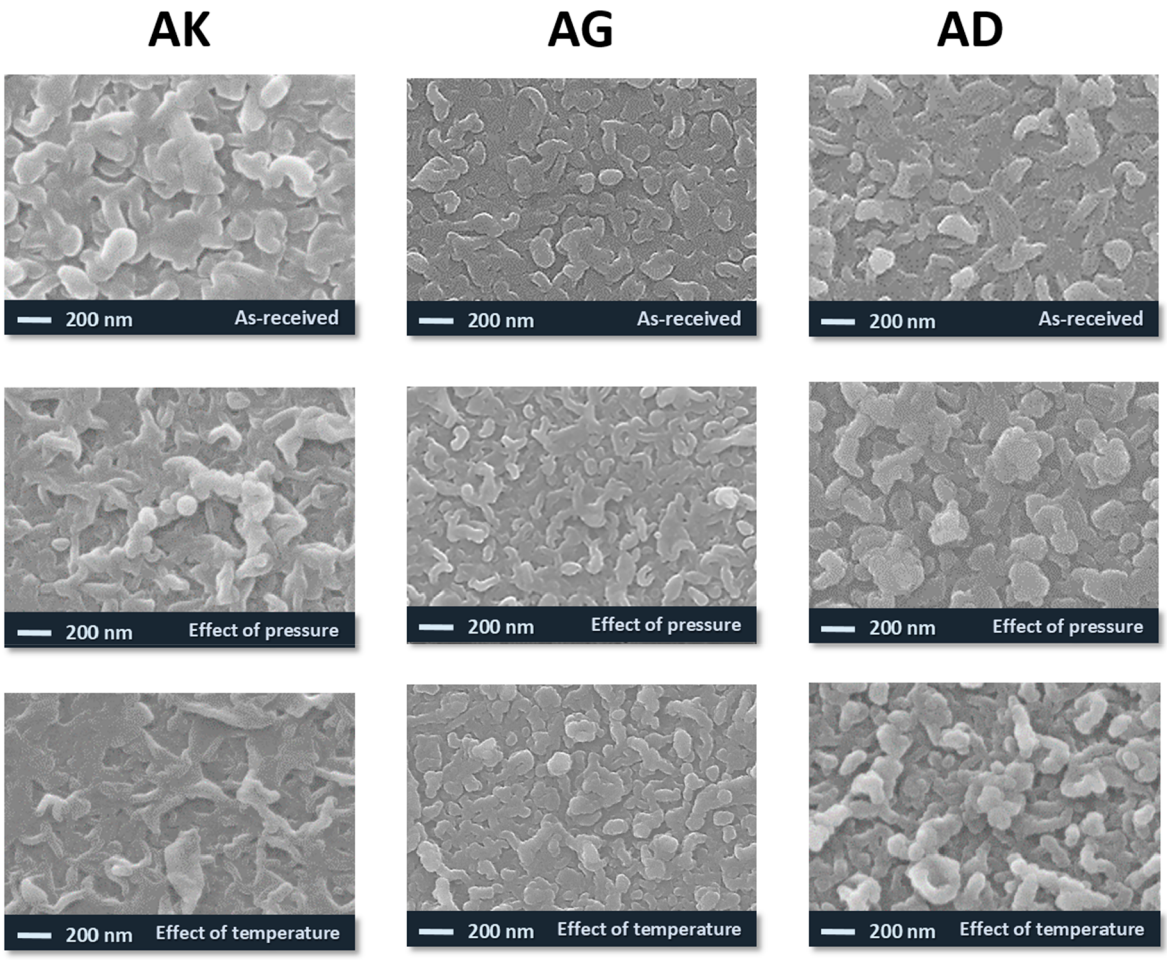

Figure 9. Top surface SEM images of as-received membranes, the membranes after filtration at room temperature, and the membranes after filtration at a high temperature.

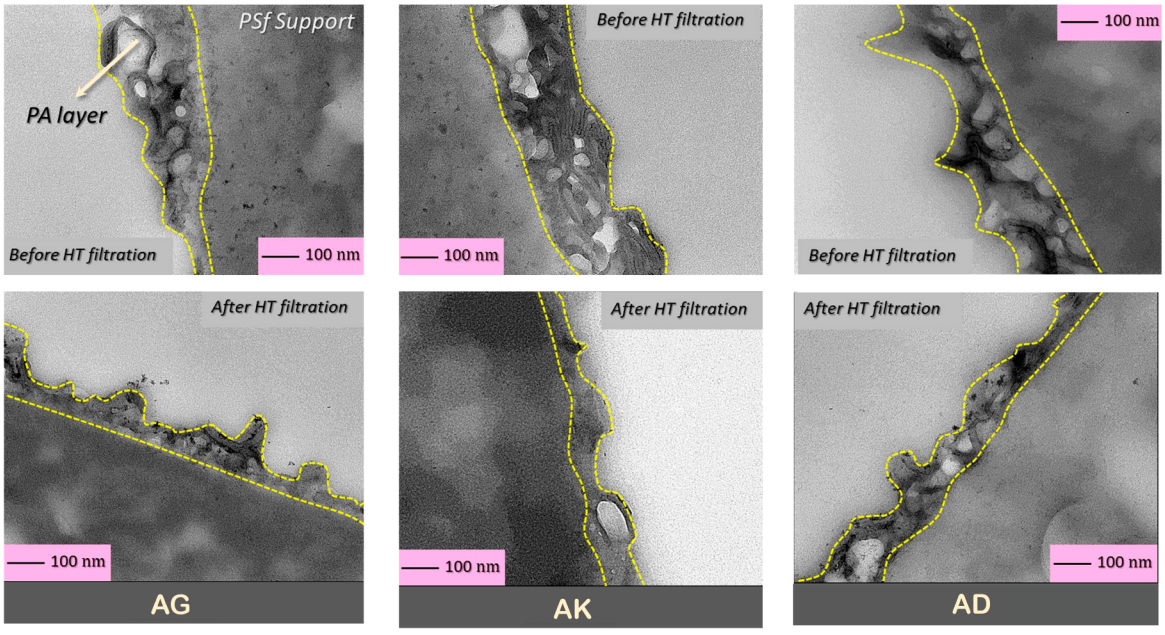

Figure 10. Cross-section TEM images of AG, AK, and AD membranes before and after high-temperature filtrations. The polyamide layer contrasts the PSf support by its spongy structure with internal voids.

temperatures. This observation is contrary to the obtained results in long-term performance and cyclic operations, in which the NaCl rejection increased at higher temperatures. By ruling out the pressure effect on the membrane at higher

https://doi.org/10.1021/acsomega.3c09331
ACS Omega 2024, 9, 1990−1999

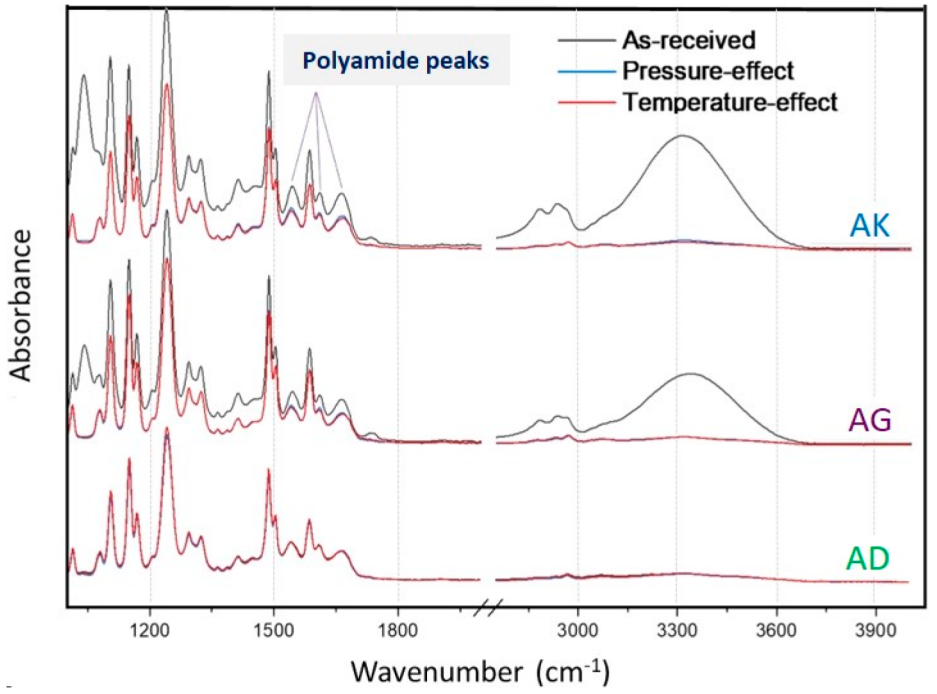

Figure 11. FTIR spectra of AG, AK, and AD membranes before and after room- and high-temperature filtrations.

temperature levels, the structural compaction of the polyamide is lower, leading to more consistent rejection results.

3.1.4. Permeability Measurement of Membranes at Different Temperatures. The pure water permeability of the TFC RO membranes at different temperatures was measured by varying the transmembrane pressure. Figure 6 depicts the water flux of AD and AG membranes at 150, 175, 200, and 225 psi in the temperature range 25−75 °C. The slope of the curve at each temperature level is the permeability of the membranes, as illustrated in the left panel of Figure 6. The permeability of the membranes (flux normalized with the pressure) was increased at elevated temperatures for both AD and AG membranes, again emphasizing the impact of temperature increment water permeation through the membrane. This result highlights that high-temperature water filtration can be more beneficial from an energy and cost-saving perspective than room-temperature water filtration.

3.1.5. Testing Membranes at Extreme Temperatures and Chemical Conditions. Despite the observed flux decline over time at elevated temperatures, a steady-state flux was reached after a certain period of time (Figures 3 and 4). Therefore, we conducted some tests under harsh chemical conditions and high temperatures to provide further insights into conditions leading to membrane failure during high-temperature filtration. Our recent findings highlight that membrane failure can occur during high-temperature filtration in the presence of chlorine in the feedwater. The performance of the AD membrane was investigated under high temperatures and the influence of chlorine. The intensified active chlorination of the polyamide selective layer at higher temperatures, illustrated in Figure 7 with 1000 ppm of sodium hypochlorite, resulted in a sudden and substantial increase in flux to over 400 LMH, accompanied by a decrease in rejection to less than 20%.

3.1.6. Effect of Temperature on the Morphological Characteristics of TFC Membranes. Figure 8 shows the top surface 3D topography AFM images of as-received membranes, the membranes after filtration at room temperature, and the membranes after filtration at high temperature. Table 1 summarizes the roughness data, including R_a (average roughness) and R_q (root-mean-square roughness).

The AK membrane exhibits a smoother surface after filtration at both room and high temperatures. In contrast, the AG membrane displays a lower variation than the AK membrane. However, the AD membrane presents a different scenario, revealing a rougher surface after filtration at elevated temperatures. This indicates that the polyamide layer of the AK membrane responds favorably to temperature changes, resulting in a decrease in surface roughness. The AG membrane, on the other hand, shows a lower variation, suggesting that its polyamide layer is less sensitive to temperature alterations compared to the AK membrane. However, the polyamide layer of the AD membrane responds adversely to higher temperatures, leading to an increase in the surface roughness. Figure 9 shows the top surface SEM images of as-received membranes, membranes after filtration at room temperature, and membranes after high temperature. As shown in Figure 9, all the images show the typical morphology of the polyamide layer: ridge-and-valley structure.[29,30] The morphology of the membranes was affected by the pressure and temperature. AK showed a less ridge-and-valley structure after filtration at elevated temperatures, consistent with the AFM results.

To further evaluate the effect of filtration temperature on the morphology and thickness of the polyamide layer, cross-sectional TEM images of reverse osmosis membranes were taken before and after high-temperature filtration. Figure 10 shows that the polyamide layer with a spongy structure containing internal voids completely covered the polysulfone (PSf) support. The internal voids in the polyamide layer are formed due to the evaporation of solvents during interfacial polymerization.[31,32]

As the filtration temperature increased, AG and AK membranes underwent significant compaction of the selective layer during long-term operation. Among them, the AK

https://doi.org/10.1021/acsomega.3c09331
ACS Omega 2024, 9, 1990−1999

membrane exhibited the most substantial structural compaction, while the AD membrane maintained nearly the same thickness of polyamide before and after high-temperature filtration. This aligns with the long-term filtration outcomes, where the AD membrane demonstrated a lower flux decline compared to that of AG and AK membranes.

3.1.7. Effect of Temperature on the Chemical Composition of TFC Membranes. Figure 11 illustrates the FTIR spectra of as-received membranes, the membranes after filtration at room temperature, and the membranes after filtration at high temperature. In AK and AG membranes, two peaks at 3350 and 1100 cm^{-1} were removed after room- and high-temperature filtration, which can be attributed to washing the preservative materials (glycerol) from the polyamide surface. The peaks at 3350 and 1100 cm^{-1} correspond to O−H stretching and alcoholic C−O asymmetric stretching vibration of glycerol, respectively.[33,34] The intensity of the peaks was also reduced after filtration for the AK and AG spectra. AD membrane exhibits the same spectra before and after high-temperature filtrations, showing high stability of the selective layer at high temperatures. From the FTIR analysis, it can be concluded that the temperature does not significantly affect the chemical composition of the polyamide layer.

4. CONCLUSION

Employing the currently available industry-standard reverse osmosis membranes for industrial and commercial high-temperature applications is still a big challenge, suggesting a high demand for the development of thermally stable membranes by modifying the chemical and morphological structures of the polyamide layer. Gaining insight into the factors influencing separation performance at elevated temperatures and establishing standardized protocols for high-temperature testing are crucial prerequisites for the development of innovative and thermally stable membranes. In this study, three commercial membranes were tested by following four different high-temperature filtration methodologies. The results showed that the brackish water membranes (AG and AK) experienced a higher flux decline during filtration at high temperatures. AD membrane as a seawater desalination membrane showed more stable performance at higher temperatures. However, fabricating highly permeable reverse osmosis membranes (like AG and AK) with robust polymeric selective layers and high thermal tolerance remains challenging since available thermally stable membranes (like AD), designed for specific applications, provide low water recovery.

AUTHOR INFORMATION

Corresponding Author

Mohtada Sadrzadeh − *Department of Mechanical Engineering, 10-367 Donadeo Innovation Center for Engineering, Advanced Water Research Lab (AWRL), University of Alberta, Edmonton, Alberta T6G 1H9, Canada;* orcid.org/0000-0002-0403-8351; Email: sadrzade@ualberta.ca

Authors

Pooria Karami − *Department of Mechanical Engineering, 10-367 Donadeo Innovation Center for Engineering, Advanced Water Research Lab (AWRL) and Department of Chemical & Materials Engineering, 12-263 Donadeo Innovation Centre for Engineering, Group of Applied Macromolecular Engineering, University of Alberta, Edmonton, Alberta T6G 1H9, Canada;* orcid.org/0000-0001-5532-6882

Sadegh Aghapour Aktij − *Department of Mechanical Engineering, 10-367 Donadeo Innovation Center for Engineering, Advanced Water Research Lab (AWRL) and Department of Chemical & Materials Engineering, 12-263 Donadeo Innovation Centre for Engineering, Group of Applied Macromolecular Engineering, University of Alberta, Edmonton, Alberta T6G 1H9, Canada;* orcid.org/0000-0002-7802-2686

Kazem Moradi − *Department of Mechanical Engineering, 10-367 Donadeo Innovation Center for Engineering, Advanced Water Research Lab (AWRL), University of Alberta, Edmonton, Alberta T6G 1H9, Canada*

Masoud Rastgar − *Department of Mechanical Engineering, 10-367 Donadeo Innovation Center for Engineering, Advanced Water Research Lab (AWRL), University of Alberta, Edmonton, Alberta T6G 1H9, Canada*

Behnam Khorshidi − *Department of Chemical Engineering and Applied Chemistry, University of Toronto, Toronto, Ontario M5S 3E5, Canada*

Farshad Mohammadtabar − *Department of Mechanical Engineering, 10-367 Donadeo Innovation Center for Engineering, Advanced Water Research Lab (AWRL), University of Alberta, Edmonton, Alberta T6G 1H9, Canada*

John Peichel − *Veolia Water Technologies & Solutions, Minnetonka, Minnesota 55343, United States*

Michael McGregor − *Suncor Energy Inc., Calgary, Alberta T2P 3E3, Canada*

Ahmad Rahimpour − *Department of Mechanical Engineering, 10-367 Donadeo Innovation Center for Engineering, Advanced Water Research Lab (AWRL), University of Alberta, Edmonton, Alberta T6G 1H9, Canada;* orcid.org/0009-0006-6658-9809

Joao B. P. Soares − *Department of Chemical & Materials Engineering, 12-263 Donadeo Innovation Centre for Engineering, Group of Applied Macromolecular Engineering, University of Alberta, Edmonton, Alberta T6G 1H9, Canada;* orcid.org/0000-0001-8017-143X

Complete contact information is available at: https://pubs.acs.org/10.1021/acsomega.3c09331

Notes

The authors declare no competing financial interest.

ACKNOWLEDGMENTS

The authors would like to thank Suncor Energy, Inc. and Canadian Natural Resources Limited (CNRL), and Veolia Water Technologies & Solutions for financially and technically supporting this project. The authors acknowledge Emissions Reduction Alberta for funding our High-Temperature Reverse Osmosis (HTRO) project.

REFERENCES

(1) Shen, J.; Richards, B. S.; Schäfer, A. I. Renewable energy powered membrane technology: Case study of St. Dorcas borehole in Tanzania demonstrating fluoride removal via nanofiltration/reverse osmosis. *Sep. Purif. Technol.* **2016**, *170*, 445−452.

(2) Karami, P.; Khorshidi, B.; McGregor, M.; Peichel, J. T.; Soares, J. B. P.; Sadrzadeh, M. Thermally stable thin film composite polymeric membranes for water treatment: A review. *J. Clean. Prod.* **2020**, *250*, 119447.

https://doi.org/10.1021/acsomega.3c09331
ACS Omega 2024, 9, 1990−1999

(3) Atallah, C.; Tremblay, A. Y.; Mortazavi, S. Silane surface modified ceramic membranes for the treatment and recycling of SAGD produced water. *J. Pet. Sci. Eng.* **2017**, *157*, 349−358.
(4) Hayatbakhsh, M.; Sadrzadeh, M.; Pernitsky, D.; Bhattacharjee, S.; Hajinasiri, J. Treatment of an in situ oil sands produced water by polymeric membranes. *Desalin. Water Treat.* **2016**, *57*, 14869−14887.
(5) Jian, X.; Dai, Y.; He, G.; Chen, G. Preparation of UF and NF poly (phthalazine ether sulfone ketone) membranes for high temperature application. *J. Membr. Sci.* **1999**, *161*, 185−191.
(6) Chu, H. C.; Campbell, J. S.; Light, W. G. High-temperature reverse osmosis membrane element. *Desalination.* **1988**, *70*, 65−76.
(7) Khorshidi, B.; Biswas, I.; Ghosh, T.; Thundat, T.; Sadrzadeh, M. Robust fabrication of thin film polyamide-TiO 2 nanocomposite membranes with enhanced thermal stability and anti-biofouling propensity. *Sci. Rep.* **2018**, *8*, 784.
(8) Rastgar, M.; Shakeri, A.; Karkooti, A.; Asad, A.; Razavi, R.; Sadrzadeh, M. Removal of trace organic contaminants by melamine-tuned highly crosslinked polyamide TFC membranes. *Chemosphere.* **2020**, *238*, No. 124691.
(9) Shaffer, D. L.; Tousley, M. E.; Elimelech, M. Influence of polyamide membrane surface chemistry on gypsum scaling behavior. *J. Membr. Sci.* **2017**, *525*, 249−256.
(10) Aghaei, A.; Firouzjaei, M. D.; Karami, P.; Aktij, S. A.; Elliott, M.; Mansourpanah, Y.; Rahimpour, A.; Soares, J. B. P.; Sadrzadeh, M. The implications of 3 D-printed membranes for water and wastewater treatment and resource recovery. *Can. J. Chem. Eng.* **2022**, *100*, 2309−2321.
(11) Elimelech, M.; Phillip, W. a The future of seawater desalination: energy, technology, and the environment. *Science (80-.).* **2011**, *333*, 712−717.
(12) Karami, P.; Aktij, S. A.; Khorshidi, B.; Firouzjaei, M. D.; Asad, A.; Elliott, M.; Rahimpour, A.; Soares, J. B. P.; Sadrzadeh, M. Nanodiamond-decorated thin film composite membranes with antifouling and antibacterial properties. *Desalination.* **2022**, *522*, No. 115436.
(13) Firouzjaei, M. D.; Seyedpour, S. F.; Aktij, S. A.; Giagnorio, M.; Bazrafshan, N.; Mollahosseini, A.; Samadi, F.; Ahmadalipour, S.; Firouzjaei, F. D.; Esfahani, M. R.; et al. others, Recent advances in functionalized polymer membranes for biofouling control and mitigation in forward osmosis. *J. Membr. Sci.* **2020**, *596*, No. 117604.
(14) Khorshidi, B.; Thundat, T.; Pernitsky, D.; Sadrzadeh, M. A parametric study on the synergistic impacts of chemical additives on permeation properties of thin film composite polyamide membrane. *J. Membr. Sci.* **2017**, *535*, 248−257.
(15) Mänttäri, M.; Pihlajamäki, A.; Kaipainen, E.; Nyström, M. Effect of temperature and membrane pre-treatment by pressure on the filtration properties of nanofiltration membranes. *Desalination.* **2002**, *145*, 81−86.
(16) Sadrzadeh, M.; Hajinasiri, J.; Bhattacharjee, S.; Pernitsky, D. Nanofiltration of oil sands boiler feed water: Effect of pH on water flux and organic and dissolved solid rejection. *Sep. Purif. Technol.* **2015**, *141*, 339−353.
(17) Roy, Y.; Warsinger, D. M.; Lienhard, J. H. others, Effect of temperature on ion transport in nanofiltration membranes: Diffusion, convection and electromigration. *Desalination.* **2017**, *420*, 241−257.
(18) Roy, Y.; Lienhard, J. H. Factors contributing to the change in permeate quality upon temperature variation in nanofiltration. *Desalination.* **2019**, *455*, 58−70.
(19) Karami, P.; Khorshidi, B.; Soares, J. B. P.; Sadrzadeh, M. Fabrication of Highly Permeable and Thermally-Stable Reverse Osmosis Thin Film Composite Polyamide Membranes. *ACS Appl. Mater. Interfaces.* **2020**, *12*, 2916−2925.
(20) Karami, P.; Khorshidi, B.; Shamaei, L.; Beaulieu, E.; Soares, J. B. P.; Sadrzadeh, M. Nanodiamond-Enabled Thin-Film Nanocomposite Polyamide Membranes for High-Temperature Water Treatment. *ACS Appl. Mater. Interfaces.* **2020**, *12*, 53274−53285.
(21) Rezakazemi, M.; Sadrzadeh, M.; Matsuura, T. Thermally stable polymers for advanced high-performance gas separation membranes. *Prog. Energy Combust. Sci.* **2018**, *66*, 1−41.
(22) Wei, J.; Jian, X.; Wu, C.; Zhang, S.; Yan, C. Influence of polymer structure on thermal stability of composite membranes. *J. Membr. Sci.* **2005**, *256*, 116−121.
(23) Khorshidi, B.; Biswas, I.; Ghosh, T.; Thundat, T.; Sadrzadeh, M. Robust fabrication of thin flm polyamide-TiO2 nanocomposite membranes with enhanced thermal stability and anti-biofouling propensity. *Sci. Rep.* **2018**, *8* (784), 1−10.
(24) Rajaeian, B.; Rahimpour, A.; Tade, M. O.; Liu, S. Fabrication and characterization of polyamide thin film nanocomposite (TFN) nanofiltration membrane impregnated with TiO 2 nanoparticles. *Desalination.* **2013**, *313*, 176−188.
(25) Wu, H.; Tang, B.; Wu, P. MWNTs/polyester thin film nanocomposite membrane: an approach to overcome the trade-off effect between permeability and selectivity. *J. Phys. Chem. C* **2010**, *114*, 16395−16400.
(26) Guan, S.; Zhang, S.; Han, R.; Zhang, B.; Jian, X. Preparation and properties of novel sulfonated copoly (phthalazinone biphenyl ether sulfone) composite nanofiltration membrane. *Desalination.* **2013**, *318*, 56−63.
(27) Al-Mutaz, I. S.; Al-Ghunaimi, M. A.Performance of Reverse Osmosis Units at High Temperatures. *Proceedings of the IDA World Congress on Desalination and Water Reuse*. Bahrain, Oct. 26−31, 2001
(28) Snow, M. J. H.; de Winter, D.; Buckingham, R.; Campbell, J.; Wagner, J. New techniques for extreme conditions: high temperature reverse osmosis and nanofiltration. *Desalination.* **1996**, *105*, 57−61.
(29) Shamaei, L.; Karami, P.; Khorshidi, B.; Farnood, R.; Sadrzadeh, M. Novel Lignin-Modified Forward Osmosis Membranes: Waste Materials for Wastewater Treatment. *ACS Sustain. Chem. Eng.* **2021**, *9*, 15768−15779.
(30) Perera, D. H. N.; Song, Q.; Qiblawey, H.; Sivaniah, E. Regulating the aqueous phase monomer balance for flux improvement in polyamide thin film composite membranes. *J. Membr. Sci.* **2015**, *487*, 74−82.
(31) Karami, P.; Khorshidi, B.; Soares, J. B. P.; Sadrzadeh, M. Fabrication of Highly Permeable and Thermally-Stable Reverse Osmosis Thin Film Composite Polyamide Membranes. *ACS Appl. Mater. Interfaces.* **2020**, *12* (2), 2916−2925.
(32) Ma, X.-H.; Yao, Z.-K.; Yang, Z.; Guo, H.; Xu, Z.-L.; Tang, C. Y.; Elimelech, M. Nanofoaming of Polyamide Desalination Membranes To Tune Permeability and Selectivity. *Environ. Sci. Technol. Lett.* **2018**, *5*, 123−130.
(33) Karami, P.; Mizan, M. M. H.; Ammann, C.; Taghipour, A.; Soares, J. B. P.; Sadrzadeh, M. Novel lignosulfonated polyester membranes with remarkable permeability and antifouling characteristics. *J. Membr. Sci.* **2023**, *687*, No. 122034.
(34) Esmaeili, M.; Virtanen, T.; Lahti, J.; Mänttäri, M.; Kallioinen, M. Vanillin as an antifouling and hydrophilicity promoter agent in surface modification of polyethersulfone membrane. *Membranes (Basel).* **2019**, *9*, 56.

https://doi.org/10.1021/acsomega.3c09331
ACS Omega 2024, 9, 1990−1999